CHEMISTRY
A EUROPEAN JOURNAL

DOI: 10.1002/chem.200701590

Acid-Catalyzed Nucleophilic Aromatic Substitution: Experimental and Theoretical Exploration of a Multistep Mechanism

Mårten Jacobsson,[a] Jonas Oxgaard,*[b] Carl-Olof Abrahamsson,[a] Per-Ola Norrby,*[c] William A. Goddard, III,[b] and Ulf Ellervik*[a]

Abstract: The mechanism for the acid-mediated substitution of a phenolic hydroxyl group with a sulfur nucleophile has been investigated by a combination of experimental and theoretical methods. We conclude that the mechanism is distinctively different in nonpolar solvents (i.e., toluene) compared with polar solvents. The cationic mechanism, proposed for the reaction in polar solvents, is not feasible and the reaction instead proceeds through a multistep mechanism in which the acid (*p*TsOH) mediates the proton shuffling. From DFT calculations, we found a rate-determining transition state with protonation of the hydroxyl group to generate free water and a tight ion pair between a cationic protonated naphthalene species and a tosylate anion. Kinetic experiments support this mechanism and show that, at moderate concentrations, the reaction is first order with respect to 2-naphthol, *n*-propanethiol, and *p*-toluenesulfonic acid (*p*TsOH). Experimentally determined activation parameters are similar to the calculated values ($\Delta H_{exp}^{\ddagger} = 105 \pm 9$, $\Delta H_{calcd}^{\ddagger} = 118\ kJ\,mol^{-1}$; $\Delta G_{exp}^{\ddagger} = 112 \pm 18$, $\Delta G_{calcd}^{\ddagger} = 142\ kJ\,mol^{-1}$).

Keywords: aromatic substitution · density functional calculations · kinetics · nucleophilic substitution · reaction mechanisms

Introduction

Aryl thiols and disulfides are important compounds in organic, bioorganic, and medicinal chemistry, with applications such as strong nucleophiles,[1] molecular switches,[2] chemisorption onto metal surfaces,[3] and resin-bound scavengers for electrophiles.[4] Disulfides have also been used as the active bond in dynamic combinatorial chemistry,[5] and sulfur-substituted aromatics are common in medicinal chemistry.

Aryl thiols can be synthesized in a variety of ways, for example, through the Newman–Karnes procedure[6] or by cleavage of an aryl–alkyl thioether bond by dissolving a metal reductant in liquid ammonia.[7] The necessary aryl thioethers can in turn be synthesized by the coupling of halides with thiols[8] or by acid-mediated substitution of a phenolic hydroxyl group with a thiol.[9] While the synthetic routes from aryl halides and aryl thiols are straightforward, they are hampered by the availability of the necessary aryl substrates. As part of an ongoing project aimed at hydroxynaphthyl disulfides,[9d] we explored a general synthetic route in which the first step is the synthesis of an intermediate thioether from the corresponding dihydroxynaphthalenes by acid-mediated substitution in a nonpolar solvent (i.e., toluene).

Despite the importance of thioethers, little appears to be known about nucleophilic aromatic substitution in nonpolar environments. This is an attractive route due to the availability of phenolic starting materials, and in our initial studies we decided to use the reaction of *n*-propanethiol (PrSH) and 2-naphthol (**1**) under acidic conditions (*p*-toluenesulfonic acid, *p*TsOH) as a model system (Scheme 1).

From the literature, we found that the mechanism for this reaction had not been properly investigated. In the first published work regarding the reaction, Furman et al.[9a] state that the mechanism is analogous to that of the Bucherer re-

[a] Dr. M. Jacobsson, C.-O. Abrahamsson, Dr. U. Ellervik
Organic Chemistry, Lund University
P.O. Box 124, 221 00 Lund (Sweden)
Fax: (+46) 46-2228209
E-mail: ulf.ellervik@organic.lu.se

[b] Dr. J. Oxgaard, Prof. W. A. Goddard, III
Materials Process and Simulation Center
Beckman Institute (139-74)
California Institute of Technology
Pasadena, CA 91125 (USA)

[c] Prof. P.-O. Norrby
Department of Chemistry, University of Gothenburg
Kemigården 4, 412 96 Gothenburg (Sweden)

Supporting information for this article is available on the WWW under http://www.chemeurj.org/ or from the author.

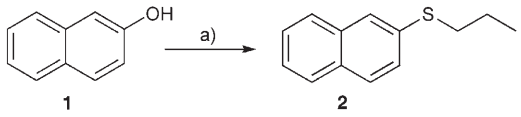

Scheme 1. The model system used in this study. a) PrSH, *p*TsOH, toluene.

action[10] (i.e., the formation of aromatic amines from phenols) and therefore formally proceeds by the formation of a hemithioketal (Scheme 2). An alternative mechanism involving attack by the thiol on a carbonium ion formed by the loss of water from the protonated naphthol was also discussed but rejected by the authors. The formation of the tautomeric keto form of naphthols under acid catalysis is well known and has been investigated both experimentally and theoretically.[11]

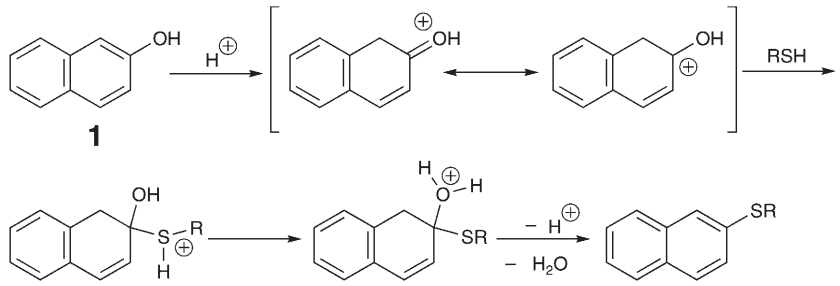

Scheme 2. Formation of a thioether from **1** as proposed by Furman et al.[9a]

The mechanism for the original Bucherer reaction has been much debated. Since the original observation of the sulfite-catalyzed interconversion of naphthol derivatives and naphthylamines by Lepetit in 1896[12] and further work by Bucherer,[10,13] several structures for the intermediates have been proposed.[14] Rieche and Seeboth studied the Bucherer reaction extensively, and proposed what is now seen as the established mechanism with addition of a bisulfite anion to C3 of the keto tautomer of the naphthol.[15] Interestingly, Seeboth reports that the sodium sulfonate of **1** (sodium 3-tetralone-1-sulfonate) can be converted into β-naphthyl sulfides.[16]

However, all these studies were performed in polar media, in which the accepted ionic mechanism is clearly feasible. As our synthetic scheme is carried out under nonpolar conditions, we were concerned that this mechanism might not be valid. Indeed, preliminary calculations on the cationic mechanism for this reaction showed that the energies of the corresponding cations are all $>200\ kJ\,mol^{-1}$ in the nonpolar solvent used. Herein, we report a combined experimental and theoretical study of this mechanism.

Results and Discussion

Initial kinetic experiments: Due to the similar spectra of **1** and of the known 2-naphthylpropyl thioether[17] (**2**) over the entire UV region, the use of stopped-flow techniques or other methods based merely on differences in the UV spectra was not feasible. We therefore turned to chromatographic separation of starting material and product. The starting concentrations of the reactants (**1**, PrSH, and *p*TsOH) were varied in three separate series of experiments, all performed at 100 °C. Analytical samples of the reactions were taken at different times and quenched by the addition of saturated aqueous $NaHCO_3$. Samples of the organic phases were then diluted and analyzed by high-performance liquid chromatography (HPLC) with an internal standard.

After an initial lag phase (5–10 min), the reactions closely followed first order in each of the reactants (naphthol and thiol). Due to the lag phase, the rate constants were not determined from the initial rate analysis, but rather by fitting to the linear parts (range optimized by F-tests) of plots of the integrated form of pseudo-second-order analysis versus time. The results are summarized in Table 1.

Table 1. Concentrations of reactants and observed pseudo-second-order rate constants.[a]

$[Reactant]_0$ [M]	Rate constant ($\times 10^5$)	$[Reactant]_0$ [M]	Rate constant ($\times 10^5$)	$[Reactant]_0$ [M]	Rate constant ($\times 10^5$)
a) Variation of $[\mathbf{1}]_0$		b) Variation of $[PrSH]_0$		c) Variation of $[p\text{TsOH}]_0$	
0.1	14.8	0.4	15.9	0.02	0.6
0.2	15.9	0.8	11.5	0.1	15.9
0.4	15.1	1.2	9.6	0.2	38.2
0.6	14.2	2.4	9.2	0.4	47.2

[a] When held constant $[\mathbf{1}]_0 = 0.2$ M, $[PrSH]_0 = 0.4$ M, and $[p\text{TsOH}]_0 = 0.1$ M.

The observed rate constants show some variation in reaction order at high concentrations, but the linearity of the plots indicates that the reaction order is pure at moderate concentrations (up to approximately 0.5 M). The acid shows the expected behavior for a catalyst; the reaction rate is linearly dependent on the concentration up to at least one equivalent of acid (0.2 M). In summary, under the standard conditions (0.1–0.4 M of all reagents), the reaction is first order in all three components.

Density functional calculations: To shed further light on the mechanism for this reaction, we turned to DFT calculations. The procedure suggested in the literature for a related mechanism involves the protonation of the naphthol by the acid (Scheme 3), generating a conjugated cation (**3**). This

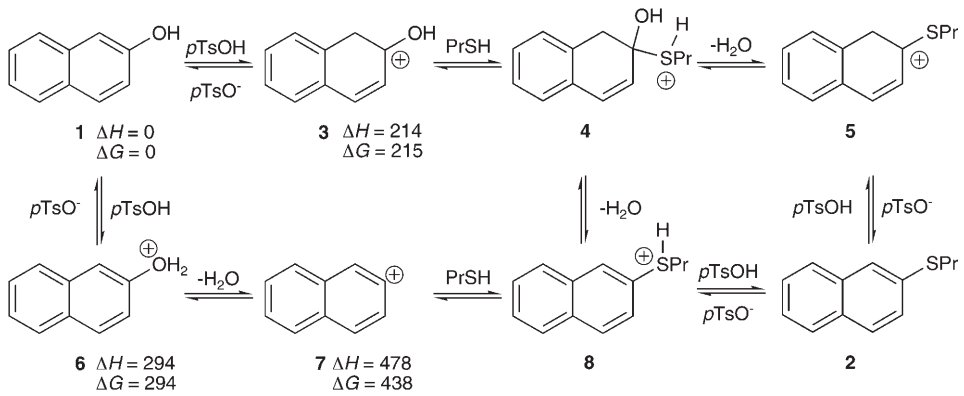

Scheme 3. Least likely cationic mechanism in nonpolar media. All energies are given in kJ mol^{-1} and are relative to the starting materials.

cation would then be attacked by the sulfur nucleophile, thus eliminating water and regenerating the acid. An alternative to this mechanism would be the protonation of the more basic OH group (to form **6**), which after elimination of H_2O would lead to a highly unlikely aryl cation (**7**). This would also undergo attack by PrSH (to give **8**) followed by regeneration of the acid (to give **2**).

However, our calculations show that none of the protonated species **3**, **6**, or **7** is energetically accessible in nonpolar media, with ΔH (ΔG) = 214 (215) kJ mol^{-1} for **3**, 294 (294) kJ mol^{-1} for **6**, and 478 (438) kJ mol^{-1} for **7**. Control calculations on these species in water lead to much more accessible energies, which suggests that this mechanism is viable in polar media, but not under the current conditions. We also explored other possible protonated isomers (**9**–**11**, Scheme 4) but, as expected, all were found to be even higher in energy than **3** (**9** and **10**) or unstable (**11** rearranged to **6** upon optimization).

Instead, we explored mechanisms that do not involve explicit protonation of the starting material (Figure 1). For reasons of consistency, we elected to keep the catalytic acid associated with the starting material throughout the calculated mechanism. In the real system, the neutral acid is expected

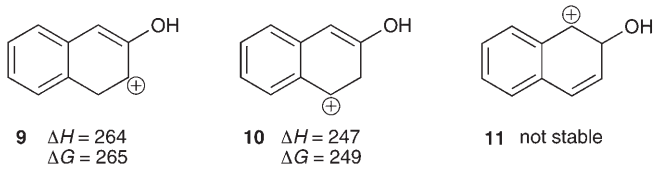

Scheme 4. Structures of **9**–**11** and calculated energies for **9** and **10**. All values are given in kJ mol^{-1}.

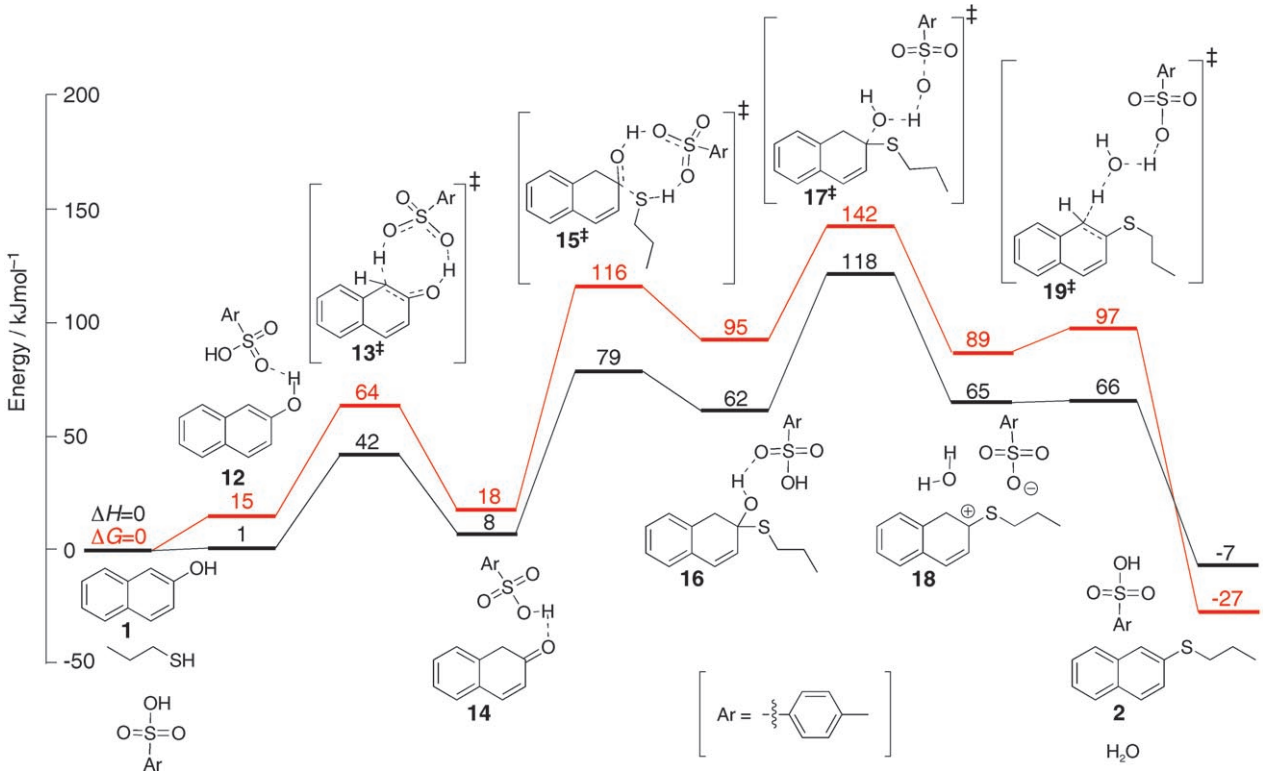

Figure 1. Calculated reaction profile: enthalpies in black, free energies in red. All energies are given in kJ mol^{-1} and are relative to the starting materials.

to rapidly dissociate and reassociate, as the energy of association is at best a few kJ mol^{-1}. We performed control calculations on the infinitely separated species for every stable neutral intermediate, and in no case was the relative energy difference between the associated and dissociated complexes more than 20 kJ mol^{-1}. In addition, many of these intermediates are flexible, and as we did not undertake an exhaustive sampling of the conformational space, it is possible that lower-energy rotamers exist other than the ones optimized. However, as all intermediates of the reaction are higher in energy than the starting materials (**1**, *p*TsOH, and PrSH), the probability of a new global ground state being introduced through rotation around bonds is small and should not influence the conclusions of this study.

As a direct nucleophilic attack on the relatively electron-rich π system in **1** is unlikely, we reasoned that the first step of the reaction should be the acid-catalyzed tautomerization of **1** to 2(1*H*)naphthone (**14**). Before the tautomerization, **1** and *p*TsOH should form a complex (**12**) which, with a relative energy of ΔH (ΔG) = 1 (15) kJ mol^{-1}, is roughly thermoneutral with the separated reagents. From **12**, a concerted transition state, **13**‡, was found for the tautomerization, with $\Delta H^{\ddagger}_{calcd}$ ($\Delta G^{\ddagger}_{calcd}$) = 42, (64) kJ mol^{-1} (Figure 2a). In **13**‡, the hydrogen from *p*TsOH is transferred to the arene, whereas the hydrogen from the OH group is transferred to one of the S=O moieties in *p*TsOH. The result of the tautomerization is **14**, which is ΔH (ΔG) = 8 (18) kJ mol^{-1} higher in energy than **1** + *p*TsOH + PrSH.

From **14**, PrSH can conduct a nucleophilic attack on the relatively positive C=O carbon atom, but only if assisted by *p*TsOH in a fairly complicated eight-centered transition state, **15**‡ (Figure 2b). In **15**‡, one hydrogen atom is transferred from *p*TsOH to the carbonyl oxygen (r(O–H) = 1.10, r(H–O) = 1.64 Å), whereas another hydrogen atom is transferred from the S–H to *p*TsOH (r(S–H) = 1.53, r(H–O) = 1.36 Å). The C–S bond is formed (r(S–C) = 2.25 Å), whereas the C=O bond is broken (r(C–O) = 1.34 Å). The two S–O bond lengths are similar (1.53 and 1.50 Å) and should be compared to the third (spectator) S=O bond length, which is 1.47 Å. The S–OH bond length in free *p*TsOH is 1.65 Å and the two S–O bonds in **15**‡ are thus clearly conjugated bonds with approximately 3/2 bond orders.

The energy of **15**‡ is calculated to be $\Delta H^{\ddagger}$ ($\Delta G^{\ddagger}$) = 79 (116) kJ mol^{-1}. The origin of the high-entropy contribution should be the requirement for three separate species to come together into an organized ring structure, of a type seldom observed for organic reactions. Only the relatively low enthalpy of the transition state allows this structure to form, and the total ΔG will rapidly increase with increasing temperature. The product of **15**‡ is structure **16**, which now has one C–OH and one C–S–*n*Pr group, and a relative energy of ΔH (ΔG) = 62 (95) kJ mol^{-1}.

Product formation occurs through a three-step mechanism that forms a very short-lived ion pair. Initially, it was expected that product formation would occur through a concerted mechanism analogous to **15**‡, but all attempts at identifying such a transition state failed and **16**, **2**, or transition-state **17**‡ resulted. It is possible that a more exhaustive scan of the reaction space could eventually lead to a concerted transition state, but considering that several attempts yielded

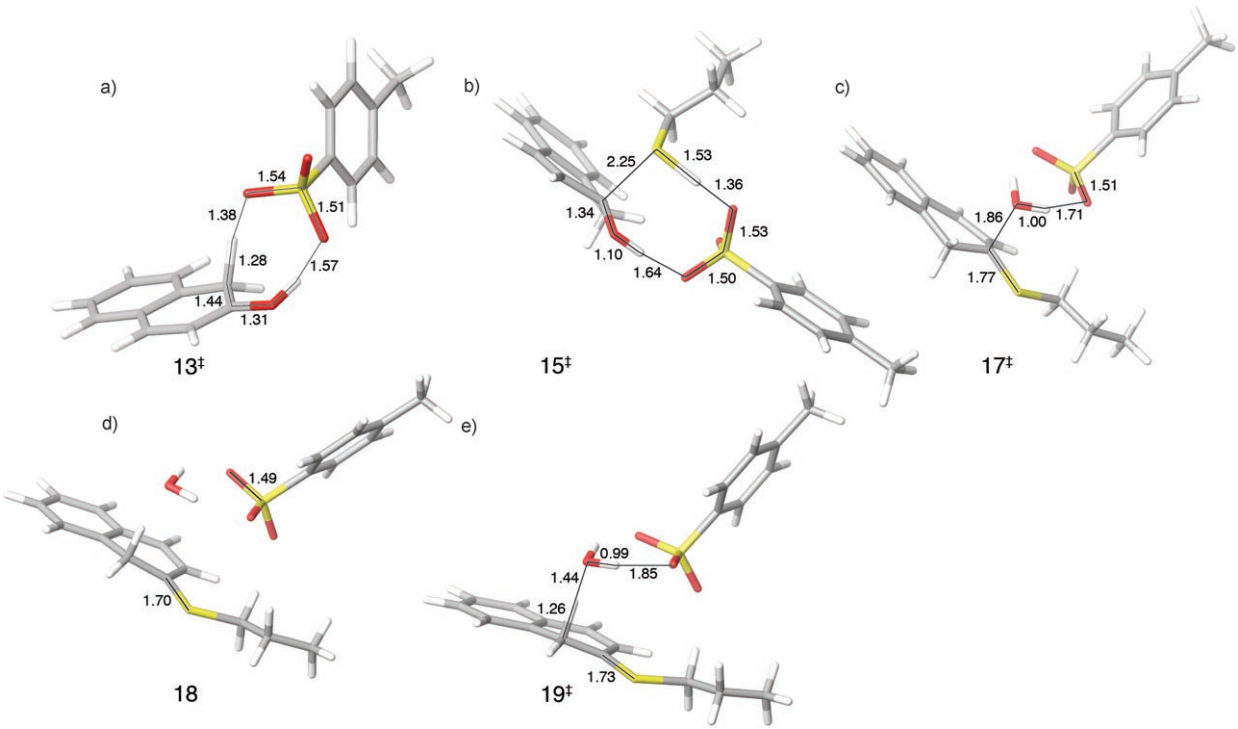

Figure 2. Structures of the transition-states **13**‡, **15**‡, **17**‡, and **19**‡ and the tight ion-pair **18**. All bond lengths are in Å.

17‡, this suggests that **17**‡ is the more favorable of the two on the ΔE surface.

The transition state we repeatedly found instead, **17**‡ (Figure 2c), is conceptually much simpler and can be described as a protonation of the ROH group to generate free water and a tight ion pair between a cationic protonated naphthalene species and a tosylate anion (**18**). **17**‡ features the transfer of the proton from *p*TsOH to the OH group ($r(O_{pTs}–H) = 1.71$ and $r(O_{OH}–H) = 1.00$ Å), which causes the C–O bond to rupture ($r(C–O) = 1.86$ Å), leading to an anion on the *p*TsOH and a cation at the 2-position on the naphthalene ring. The calculated energy of **17**‡ is ΔH (ΔG) = 118 (142) kJ mol^{-1}. While within the margin of error, we believe the calculated vibrational entropy S_{vib} is somewhat high due to an overly rigid transition state in the gas-phase optimization. In solvent, we believe that this transition state should be less rigid (as the forming charge is more efficiently stabilized), and the actual S_{vib} should consequently be somewhat higher.

The product tight ion pair (**18**, Figure 2d) features the H_2O group as a bridge between the relatively positive naphthiol proton and the tosylate anion. The energy of **18** is only ΔH (ΔG) = 65 (89) kJ mol^{-1}, which indicates a large amount of charge stabilization. The separated ions (treated as [*p*TsO:H_2O]$^-$ + [naphthiol]$^+$, [*p*TsO]$^-$ + [naphthiol:H_2O]$^+$, and [*p*TsO]$^-$ + [naphthiol]$^+$ + H_2O showed that separating the ions costs ΔH (ΔG) = 173 (183) kJ mol^{-1}, 176 (176) kJ mol^{-1}, and 196 (177) kJ mol^{-1}, respectively, that is, significantly higher energy relative to **18**. The cation in **18** is stabilized by both conjugation in the naphthalene ring and conjugation from the sulfur lone pair. Indeed, the C–S bond length in **18** is only 1.70 Å, which should be compared with 1.94 Å in **16** and 1.78 Å in the naphthyl thiol product. Consequently, this bond should most likely be considered a C=S double bond, with most of the charge localized on the sulfur atom.

From **18**, a last transition state (**19**‡, Figure 2e) leads to the products **2**, H_2O, and *p*TsOH. Transition-state **19**‡ is formed by a proton-shuffling mechanism, in which the naphtholic proton that coordinated to the H_2O in **18** is transferred to the oxygen ($r(C–H) = 1.26$ Å, $r(H–O_{OH}) = 1.44$ Å), whereas one of the protons on H_2O is transferred to the *p*TsO$^-$ anion ($r(O_{OH}–H) = 0.99$ Å, $r(H–O_{pTs}) = 1.85$ Å). The energy of **19**‡ is only ΔH (ΔG) = 66 (97) kJ mol^{-1}, that is, only marginally higher than the energy of the tight ion pair **18**. Transition-state **19**‡ produces the final products, with a relative energy of ΔH (ΔG) = −7 (−27) kJ mol^{-1}. This energy is consistent with the experimentally observed near-quantitative conversion of starting materials into product.

The complexity of this mechanism suggests that it might only work under very select conditions. A more polar solvent might stabilize **18** sufficiently so that the ions can separate in solution, which might lead to other products. Also, **15**‡ requires a chelating acid to transfer the proton efficiently, and it is thus predicted that an acid, such as HCl, must react either through an analogous six-membered transition state, a stepwise mechanism, or another tight ion pair. Any of these mechanisms might allow for unwanted side reactions, which is consistent with the experimentally observed results and indicates that HCl does give a product but the reaction does not proceed as cleanly as with *p*TsOH.

Other explored mechanisms include a concerted substitution of the OH group with *p*TsOH (Scheme 5) to generate a naphthyl–tosylate complex, which could then undergo the reverse substitution with PrSH. We hypothesized that the energy of this six-membered transition state could compare favorably to those of the eight-membered transition states shown above. However, calculations for a model system suggested a barrier for the first step of ≈232 kJ mol^{-1}, and this mechanism was not further explored.

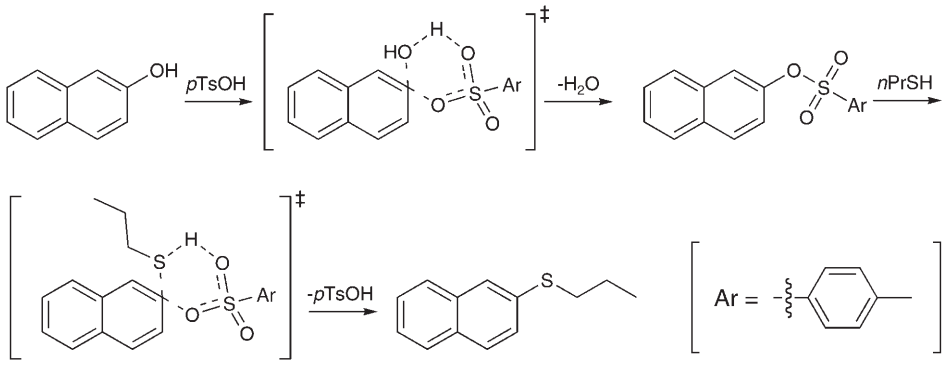

Scheme 5. Explored concerted substitution mechanism. The energy for the first transition state was ≈232 kJ mol^{-1}.

Calculations on a four-center mechanism for the process **14**→**16**, in which the S–H bond transfers a hydrogen atom directly to the C=O oxygen atom without the help of *p*TsOH, failed to find a feasible transition state. Intriguingly, several of the attempts ended up identifying a transition state for the process **12**→**14** instead, but with a calculated barrier of 133 kJ mol^{-1}. As this process has a barrier of 42 kJ mol^{-1} when using *p*TsOH as the proton-transfer agent, and since the desired pathway has a barrier of 79 kJ mol^{-1} when using *p*TsOH, one could assume that the analogous PrSH pathway has a prohibitively high barrier. Finally, several radical intermediates (analogous to the cationic intermediates **3**, **9**, **10**, and **1**), in which either *p*TsOH or PrSH acted as the hydrogen-radical donor, were calculated but all were found to have relative energies of >200 kJ mol^{-1}.

Kinetic determination of activation parameters: To support the proposed mechanism, we decided to determine the acti-

vation parameters from an Eyring plot. The model reaction was performed at 5 °C intervals from 70 to 110 °C and the rate constants (corrected for the initial concentration of *p*TsOH) were calculated as described for the initial kinetic experiments. An Eyring plot was constructed and a linear model was fitted to the data (Figure 3). The activation parameters were then calculated from the data (Table 2).

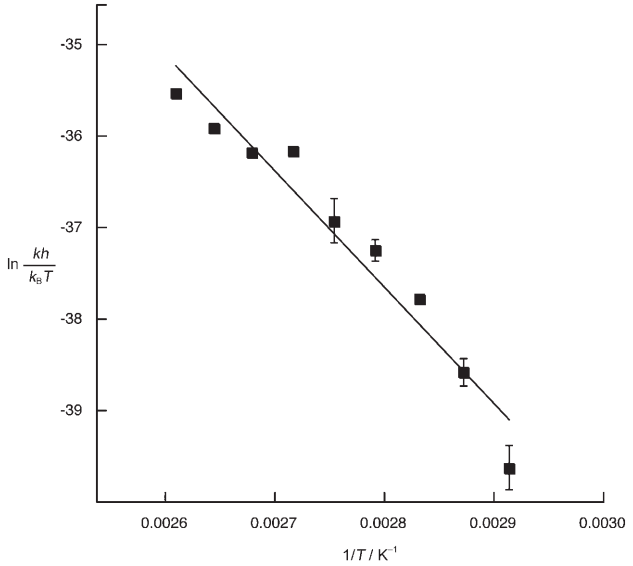

Figure 3. Eyring plot for the formation of **2**.

Table 2. Activation parameters for the formation of **2**.[a]

Parameter	Value from Eyring plot with standard error	Value from DFT calculations
$\Delta H^{\neq}$ [kJ mol^{-1}]	105 ± 9	118
$\Delta S^{\neq}$ [J mol^{-1}K]	-18 ± 26	-66[b]
$\Delta G^{\neq}$ [kJ mol^{-1}]	112 ± 18	142

[a] $\Delta G^{\neq}$ is calculated from $\Delta H^{\neq}$, and $\Delta S^{\neq}$ at 363 K. [b] Corrected value, see the Experimental Section.

Conclusion

The mechanism for the acid-catalyzed substitution of phenolic hydroxyl groups with sulfur nucleophiles is distinctively different in nonpolar solvents (i.e., toluene) compared to polar solvents. The cationic mechanism, proposed for the reaction in polar solvents, is clearly not feasible under nonpolar conditions. Instead, the reaction proceeds through a multistep mechanism in which the acid (*p*TsOH) mediates the proton shuffling. From DFT calculations we found a rate-determining transition state, with protonation of the hydroxyl group to generate free water and a tight ion pair between a cationic protonated naphthalene species and a tosylate anion. The kinetic experiments support this mechanism and show that the reaction, at moderate concentrations, is first order with respect to **1**, PrSH, and *p*TsOH. The activation parameters, extracted from an Eyring plot, back up the proposed mechanism. The $\Delta H^{\neq}$ values are similar (105 ± 9 vs. 118 kJ mol^{-1}), whereas the $\Delta G^{\neq}$ values are somewhat more disparate (112 ± 18 vs. 142 kJ mol^{-1}), which can be explained by a somewhat overestimated $\Delta S^{\neq}$ value in the gas-phase calculations compared to solvent conditions. The reaction goes to near completion, which is in accordance with the overall thermodynamics from the calculations.

Experimental Section

General: Toluene was dried by passing it through a column of Al_2O_3 (neutral, activity grade I). *p*TsOH was recrystallized from EtOAc. Preparative chromatography was performed by using silica gel (35–70 mm, 60 Å). Analytical HPLC was performed by using a HiCHROM Kromasil 100-5 sil column on a Varian ProStar system running the Varian Star chromatography workstation v.5 software.

Naphthalene-2-yl(propyl)sulfane (2):[17] 2-Napthol (**1**) (144 mg, 1 mmol), *p*TsOH (86 mg, 0.5 mmol), and PrSH (1.1 mL, 12 mmol) were suspended in toluene (5 mL) and stirred under reflux at 110 °C for 22 h. The solution was allowed to reach room temperature, washed (saturated aqueous $NaHCO_3$), dried ($MgSO_4$), filtered, and concentrated. Chromatography (silica gel, heptane/EtOAc 4:1) gave **2** as a light-yellow oil (184 mg, 91 %). The compound purity, determined by ^{1}H NMR spectroscopy and analytical HPLC, was >99 % and all spectral data were consistent with published results.

Kinetic studies: Kinetic studies were performed by adding **1**, *p*-nitrotoluene (internal standard), *p*TsOH, and PrSH (in that order) to toluene. The suspension was quickly heated to the required temperature. Samples (0.250 mL) were extracted at 0, 5, 10, 15, 30, 60, 120, 180, and 240 min and washed with saturated aqueous $NaHCO_3$ (1.5 mL). A sample of the organic phase (0.050 mL) was diluted with heptane/EtOAc (9:1, 0.90 mL) and analyzed by HPLC. For higher concentrations of product, the solution was diluted ten times before analysis. Calibration curves were acquired by analysis of the pure compounds and all integrals were normalized according to the integral of the internal standard. The stability of the internal standard to the reaction conditions was ascertained by treating it to the reaction conditions at 80 °C for 20 h followed by another 24 h at 110 °C.

Data handling and kinetic calculations: All data handling, curve fitting, and statistical analysis was performed in Microsoft Excel 2004 for Mac.

Computational chemistry: All calculations were performed by using the hybrid DFT functional B3LYP, as implemented by the Jaguar 6.5 program package.[18] This DFT functional utilizes the Becke three-parameter functional[19] (B3) combined with the correlation functional of Lee, Yang, and Parr[20] (LYP). Pople's 6-311G**++ basis set[21] was used for all gas-phase calculations and the same basis set without diffuse functions (6-311G**) for solvation calculations. Implicit solvent effects of the experimental toluene medium were calculated with the Poisson–Boltzmann (PBF) continuum approximation[22] by using the parameters $\Sigma = 2.379$ and $r_{solv} = 2.76174$ Å. Solvation effects were calculated by adding single-point solvation energies (free energies) to the energy of the gas-phase geometries. The solvation energy includes both electrostatic and nonelectrostatic interactions and can be thought of as a vertical Gibbs free energy of solvation. Whereas the solvation energies are technically ΔG terms, the ΔS component is very minor and the entire term can thus also be used to approximate ΔE and ΔH.

Consequently, all enthalpies are reported as $\Delta H(0\,\mathrm{K}) = \Delta E$ + zero-point energy (ZPE) correction + solvation correction. Free energies are calculated as $\Delta G(363\,\mathrm{K}) = \Delta H(363\,\mathrm{K}) - T\Delta S(363\,\mathrm{K})$, in which $\Delta H = \Delta E$(gas phase) + ΔE(solvation correction) + ZPE + ΔH(vib) + $3kT^*\Delta(n)$. The last term, $3kT$, is a fixed value for the sum of the rotational and translational contributions to the enthalpy at 363 K, calculated to be 9.0598 kJ mol^{-1}. The ΔS terms were calculated by the sum ΔS(vib) + ΔS(trans/rot) + ΔS(concn). ΔS(vib) is calculated from a modified Jaguar gas-phase analytical frequency calculation (see below) by using the harmonic oscillator

approximation, whereas ΔS(trans/rot) is given a fixed value of 125.4 J mol^{-1} K. The use of $3kT$ and 125.4 J mol^{-1} K for the ΔH(trans/rot) and ΔS(trans/rot) terms, respectively, was made to avoid the values obtained in the gas-phase calculations of thermodynamic properties. For a solvated reaction, these gas-phase values are substantially inflated,[23] and accurate values most likely require a full dynamic simulation. As this is outside the scope of this paper, we elected to use a fixed value reflecting the experimental value for a pure liquid. For ΔS(vib), we assumed no frequencies below 50 cm^{-1}, as the inertia of a solvent should prevent these modes from being sufficiently flexible. Consequently, frequency modes below 50 cm^{-1} were assigned as $S = 50$ cm^{-1}, and the total ΔS(vib) was calculated according to the harmonic oscillator approximation. Notably, even though the treatment of ΔH(trans/rot), ΔS(trans/rot), and ΔS(vib) contains empirical terms, the fixed parameters were assigned before analysis of the results. Thus, no fitting of parameters was performed to allow the results to correspond to experimental values. That said, we do expect the ΔG errors with this methodology to be quite large, and the actual values are most likely only qualitatively correct.

All geometries were optimized and evaluated for the correct number of imaginary frequencies through vibrational frequency calculations by using the analytic Hessian. Zero imaginary frequencies correspond to a local minimum, whereas one imaginary frequency corresponds to a transition structure.

Acknowledgement

This work was supported by The Swedish Research Council, The Crafoord Foundation, and the Chevron–Texaco Energy Research & Technology Company. Caltech computational facilities were supported by ARO-DURIP and ONR-DURIP funds. We are indebted to the Division of Undergraduate Education at the Department of Chemistry, Lund University, for the use of instruments. We thank Dr. Robert Nielsen for valuable discussions regarding thermodynamics in solution and Dr. Morten Krogh and Rickard Elmqvist for valuable discussions regarding statistics.

[1] K. A. Stubbs, M. S. Macauley, D. J. Vocadlo, *Carbohydr. Res.* **2006**, *341*, 1764–1769.
[2] H. Röhr, C. Trieflinger, K. Rurack, J. Daub, *Chem. Eur. J.* **2006**, *12*, 689–700.
[3] R. R. Kolega, J. B. Schlenoff, *Langmuir* **1998**, *14*, 5469–5478.
[4] S. V. Ley, A. Massi, *J. Chem. Soc. Perkin Trans. 1* **2000**, *21*, 3645–3654.
[5] J.-M. Lehn, *Chem. Eur. J.* **1999**, *5*, 2455–2463.
[6] M. S. Newman, H. A. Karnes, *J. Org. Chem.* **1966**, *31*, 3980–3984.
[7] a) G. K. Hughes, E. O. P. Thompson, *J. Proc. R. Soc. N. S. W.* **1948**, *82*, 262–264; b) R. Adams, A. Ferretti, *J. Am. Chem. Soc.* **1959**, *81*, 4939–4940; c) A. Ferretti, *Organic Syntheses, Vol. 5*, Wiley, New York, **1973**, pp. 419–421; d) R. Gleiter, J. Uschmann, *J. Org. Chem.* **1986**, *51*, 370–380.
[8] a) R. Adams, W. Reifschneider, A. Ferretti, *Organic Syntheses, Vol. 5*, Wiley, New York, **1973**, pp. 107–110; b) P. K. Fraser, S. Woodward, *Chem. Eur. J.* **2003**, *9*, 776–783.
[9] a) F. M. Furman, J. H. Thelin, D. W. Hein, W. B. Hardy, *J. Am. Chem. Soc.* **1960**, *82*, 1450–1452; b) T. Nakazawa, N. Hirose, K. Itabashi, *Synthesis* **1989**, 955–957; c) P. Charoonniyomporn, T. Thongpanchang, S. Witayakran, Y. Thebtaranonth, K. E. S. Phillips, T. J. Katz, *Tetrahedron Lett.* **2004**, *45*, 457–459; d) M. Jacobsson, U. Ellervik, K. Mani, *Bioorg. Med. Chem.* **2007**, *15*, 5283–5299.
[10] H. T. Bucherer, *J. Prakt. Chem.* **1904**, *69*, 49–91.
[11] a) *Rodd's Chemistry of Carbon Compounds, Vol. III: Aromatic Compounds, Part G* (Ed.: S. Coffey), Elsevier, Amsterdam, **1978**; b) A. V. Golounin, Y. S. Shchedron, V. A. Fedorov, *Russ. J. Org. Chem.* **2001**, *37*, 1111–1113; c) A. V. Golounin, Y. S. Shchedron, E. A. Ivanova, *Russ. J. Org. Chem.* **2001**, *37*, 1270–1272.
[12] R. Lepetit. *Bull. Soc. Ind. Mulhouse* **1903**, 326–328.
[13] H. T. Bucherer, *J. Prakt. Chem.* **1904**, *69*, 345–364.
[14] a) N. N. Woroshtzow, *J. Russ. Phys. Chem. Soc.* **1915**, *47*, 1669; b) T. Nakazawa, N. Hirose, K. Itabashi, *Synthesis* **1989**, 955–957; c) W. Fuchs, W. Stix, *Ber. Dtsch. Chem. Ges.* **1922**, *55*, 658–670; d) F. Raschig, W. Prahl, *Annalen* **1926**, *448*, 265–331.
[15] a) A. Rieche, H. Seeboth, *Liebigs Ann. Chem.* **1960**, *638*, 43–110; b) H. Seeboth, *Angew. Chem.* **1967**, *79*, 329–340; *Angew. Chem. Int. Ed. Engl.* **1967**, *6*, 307–317.
[16] See reference [15b], p. 314.
[17] See, for example: P. Pitchen, E. Duñach, M. N. Deshmukh, H. B. Kagan, *J. Am. Chem. Soc.* **1984**, *106*, 8188–8193.
[18] Jaguar 6.5, Schrodinger, Inc., Portland, Oregon, **2005**.
[19] A. D. Becke, *J. Chem. Phys.* **1993**, *98*, 5648–5652.
[20] C. Lee, W. Yang, R. G. Parr, *Phys. Rev. B* **1988**, *37*, 785–789.
[21] a) P. C. Hariharan, J. A. Pople, *Chem. Phys. Lett.* **1972**, *16*, 217–219; b) M. M. Francl, W. J. Pietro, W. J. Hehre, J. S. Binkley, M. S. Gordon, D. J. DeFrees, J. A. Pople, *J. Chem. Phys.* **1982**, *77*, 3654–3665.
[22] a) D. J. Tannor, B. Marten, R. Murphy, R. A. Friesner, D. Sitkoff, A. Nicholls, M. Ringnalda, W. A. Goddard III, B. Honig, *J. Am. Chem. Soc.* **1994**, *116*, 11875–11882; b) B. Marten, K. Kim, C. Cortis, R. A. Friesner, R. B. Murphy, M. N. Ringnalda, D. Sitkoff, B. Honig, *J. Phys. Chem.* **1996**, *100*, 11775–11788.
[23] a) T. N. Truong, T. T. Truong, E. V. Stefanovich, *J. Chem. Phys.* **1997**, *107*, 1881–1889; b) C. J. Cramer, D. G. Thrular, *Chem. Rev.* **1999**, *99*, 2161–2200.

Received: October 9, 2007
Published online: March 20, 2008

